

# Numerical Simulation of Time-Dependent Heat Transfer in Oscillating Pipe Flow

J. G. Zhang\* and U. H. Kurzweg†  
University of Florida, Gainesville, Florida 32611

The problem of Enhanced Axial Heat Transfer (EAHT) in oscillatory pipe flow has been numerically studied. Time-dependent velocity and temperature profiles and Lagrangian and tidal displacements at various Womersley numbers are obtained. The enhanced axial heat flux for different tidal displacements is calculated. The wall thickness effect in EAHT is also studied, and the optimum wall thickness is shown to be about 20% of the pipe radius in the test case studied. In addition, the tuning effect in axial heat flow is examined, the results indicating good agreement with analytic predictions. The numerical studies show that EAHT can be a very effective tool for those problems in which a large amount of heat must be transported without an accompanying convective mass exchange.

## Introduction

**E**NHANCED Axial Heat Transfer (EAHT) in viscous fluids subjected to sinusoidal oscillations in conduits has been studied analytically by Kurzweg for a 1-D time-periodic model.<sup>1-4</sup> His results show that the axial heat transferred in such oscillating flows can be orders of magnitude larger than that obtained by pure molecular conduction, and this was verified by some later experimental measurements by Kurzweg and Zhao in 1984.<sup>5</sup> The interesting feature is that the entire heat transfer process involves no net convective mass transport. Discovery of this transport process was made possible by earlier studies on axial dispersion of contaminants within steady laminar flows through capillary tubes by Taylor,<sup>6</sup> and in oscillatory laminar flows by Aris,<sup>7</sup> Harris,<sup>8</sup> and Chatwin.<sup>9</sup> In 1983, it was suggested that a similar dispersion process should occur in the heat transfer area because of the similarity of the governing equations.<sup>1</sup>

Figure 1 shows a schematic model of an EAHT device. It is assumed that a bundle of small diameter open-ended tubes is connected to a reservoir that supplies unlimited hot liquid at one end to a second reservoir that, in turn, supplies unlimited cold liquid at the other end. The liquid in the pipes is oscillated axially with an axial excursion, such that none of the liquid originally at the half-way point along the pipes ever enters either reservoir. This oscillatory motion leads to very large axial time-averaged heat flows, which can be readily made to exceed those possible with heat pipes.<sup>1</sup>

The analytical aspects of this oscillatory-enhanced axial heat transfer process have been developed much further than the experimental and numerical counterparts. Moreover, the earlier theoretical predictions are quite limited and consider only one-dimensional cases involving a number of simplifying assumptions. The present numerical study extends the analytical investigation on thermal pumping to a more complex two-dimensional axisymmetric geometry, and allows the consideration of axially dependent heat exchange between the oscillating fluid and the bounding wall with various thermal properties. Such problems cannot be handled analytically. A

detailed numerical study is, thus, crucial before further prototype designs for this kind of axial heat transfer device are undertaken. Since the pipes connecting the reservoirs play a very important role in EAHT, we will focus our attention here on the oscillatory laminar time-dependent motion in a single pipe. The problem will be considered as an initial value problem for various thermal input conditions at the pipe extremities.

## Parameters and Heat Transfer Mechanism

Before carrying out numerical calculations on the EAHT mechanism, some new terms encountered in this type of oscillatory motion need to be introduced.

### Womersley Number $\alpha$

The dimensionless parameter termed the Womersley Number is defined as  $\alpha = R_1(\omega/\nu)^{1/2}$ , where  $R_1$  is the pipe inner radius,  $\omega$  is the angular oscillating frequency, and  $\nu$  is the kinematic viscosity of the working fluid. It measures the ratio of inertial to viscous forces.

### Tidal Displacement $\Delta x$

For most EAHT applications, it is convenient to use the concept of tidal displacement  $\Delta x$ , which is defined by

$$\Delta x = \frac{2}{R_1^2} \int_0^{R_1} X\left(r, \frac{\pi}{\omega}\right) r dr \quad (1)$$

where  $X(r, \pi/\omega)$  is the Lagrangian displacement of the fluid particles at various radial positions within the capillary tube at  $t = \pi/\omega$ . It is assumed that these elements are initially lined up at axial position  $x = L/2$ , halfway between the tube ends.

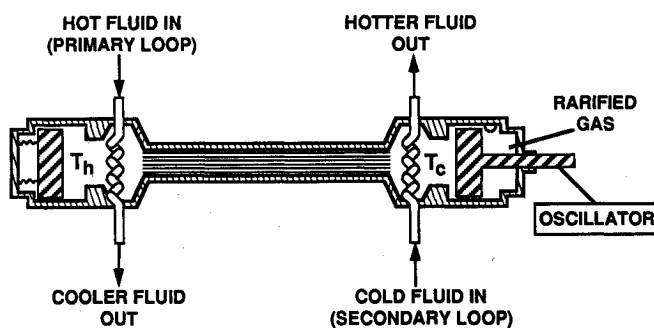


Fig. 1 Enhanced axial heat transfer device.

Received March 19, 1990; presented as Paper 90-1774 at the AIAA/ASME 5th Joint Thermophysics and Heat Transfer Conference, Seattle, WA, June 18-20, 1990; revision received Sept. 5, 1990; accepted for publication Sept. 7, 1990. Copyright © 1990 by the American Institute of Aeronautics and Astronautics, Inc. All rights reserved.

\*Presently, Post-Doctoral Fellow at Innovative Nuclear Space Power Institute (INSPI). Member AIAA.

†Professor, Department of Aerospace Engineering, Mechanics, and Engineering Science.

As a function of time  $t$  and radial distance  $r$ , the dimensional Lagrangian displacement can be computed from

$$X(r, t) = \int_0^t U(r, t) dt \quad (2)$$

where  $U(r, t)$  is the time-dependent velocity profile, which can be obtained numerically or analytically by solving the governing Equation (3). One can see that, physically, the tidal displacement  $\Delta x$  represents the maximum cross stream averaged axial excursion of fluid elements during one oscillation cycle, and is a convenient alternative to the use of a time-dependent axial pressure gradient for describing axial fluid oscillations.

#### Boundary-layer Thickness $\delta$

The Stokes viscous boundary-layer thickness is given by  $\delta = (2\nu/\omega)^{1/2}$ , and the corresponding thermal boundary-layer thickness is  $\delta_{th} = \delta/(Pr)^{1/2}$ , where  $Pr = \nu/\kappa$  is the Prandtl number.

With the definition of these quantities, we are now in a position to explore the mechanisms that make oscillatory-enhanced axial heat transfer possible. Suppose at  $t = 0$  the liquid in the pipes starts to oscillate axially. The amplitude of the oscillatory motion can be controlled by adjusting the periodic pressure difference between the two ends. After a short transient, this oscillatory motion creates a thin boundary layer and a corresponding large time-dependent radial temperature gradient that is superimposed on the existing imposed axial temperature gradient. This results in a large amount of heat being exchanged by conduction between the fluid core and the boundary layer, as well as the solid wall. In turn, the periodic interaction of axial convection with this radial conduction heat flow between the fluid core and Stokes boundary layer produces a time-averaged net heat transport from the hot end of the pipe to the cold end. The heated fluid core is partially ejected into the cold reservoir and mixed there with the lower temperature liquid. At the same time, the cooled fluid core near the hot end is periodically injected into the hot reservoir. This "thermal pumping" leads to an effective axial conductivity orders of magnitude larger than that achievable by axial conduction in the absence of oscillations. Typically, when using water as the working fluid, increases of some four orders of magnitude are found to be achievable,<sup>5</sup> without an accompanying convective mass exchange.

#### Governing Equations

The use of a circular capillary tube model with constant cross-sectional area and the neglect of the end effects allows a laminar axisymmetric 1-D time-dependent description of the flow field and a corresponding 2-D description of the oscillatory thermal field. Figure 2 shows the two model geom-

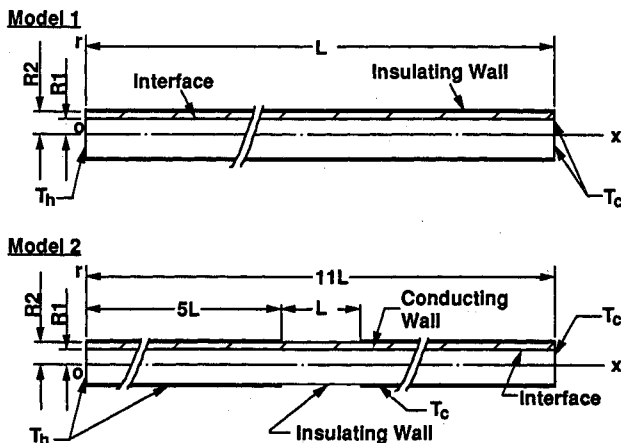


Fig. 2 Numerical models.

etries used in this study, where the tube length  $L = 20$  cm and the inner radius  $R_1 = 0.1$  cm in both cases. In the first model, the tube is directly connected to a hot fluid reservoir at  $x = 0$  and a cold reservoir at  $x = L$ . The temperature at the pipe ends are equal to  $T_h$  and  $T_c$ , and the temperature along the pipe wall satisfies insulating boundary conditions. The second model attempts to improve the heat transfer efficiency at the pipe ends by extending the pipe by  $5L$  on both ends and assuming the temperatures at the outer surface of the extended portion of the pipe to be kept constant and equal to  $T_h$  and  $T_c$ , respectively. The connecting wall can be either conducting or insulating. The continuity condition of temperature and radial heat flux must be satisfied along the inner boundaries of the pipe in both cases.

The pressure gradient induced by moving the piston shown in Fig. 1 is assumed to be harmonic and has the form  $(dp/dx) = \rho A \cos \omega t$ , where  $A$  is a constant. The simplified Navier-Stokes equation and corresponding governing heat conduction equations for the problem assume the form

$$\frac{\partial U}{\partial t} = A \cos(\omega t) + \frac{\nu}{r} \frac{\partial}{\partial r} \left[ r \left( \frac{\partial U}{\partial r} \right) \right] \quad 0 < r < R_1 \quad (3)$$

$$\frac{\partial T}{\partial t} = -U \frac{\partial T}{\partial x} + \kappa_f \left[ \frac{1}{r} \frac{\partial}{\partial r} \left( r \frac{\partial T}{\partial r} \right) + \frac{\partial^2 T}{\partial x^2} \right] \quad 0 < r < R_1 \quad (4)$$

$$\frac{\partial T}{\partial t} = \kappa_w \left[ \frac{1}{r} \frac{\partial}{\partial r} \left( r \frac{\partial T}{\partial r} \right) + \frac{\partial^2 T}{\partial x^2} \right] \quad R_1 < r < R_2 \quad (5)$$

where  $U(r, t)$  is, again, the axial velocity, and  $T(x, r, t)$  is the temperature. Also,  $R_1, R_2$  are the inner and outer radii of the tube,  $\kappa_f = k_f/\rho c$ ,  $\kappa_w = k_w/\rho_w c_w$  are the fluid and wall thermal diffusivities, and  $\rho$  and  $\rho_w$ ,  $c$  and  $c_w$  are the fluid and wall densities and specific heats, respectively. Note that the viscous heating term has been neglected in Eq. (4), since it is very small for most experimental conditions. This neglect is justified provided one does not deal with very high Prandtl number fluids such as oils. Also, Eq. (3) does not contain nonlinear convective terms, in view of the wall parallel flow existing in tubes of constant diameter and infinite length, and considers only incompressible flow.

These second-order parabolic type of governing Equations (3), (4), and (5), together with the appropriate boundary conditions, can be nondimensionalized and transformed from the physical domain into a computational domain. This was done in the present study. The implicit unconditional stable Crank-Nicolson scheme and the Alternating Direction Implicit (ADI) method were employed to break up the transformed equations into finite-difference form. A variable grid network, in which the grid-lines are clustered within the expected boundary-layer regions near the tube wall, was used to insure a higher resolution of the thermal and flow variables (see Zhang<sup>10</sup> for details).

#### Results and Discussion

The results of the study include two parts: oscillatory features of the flow and temperature fields, and numerical results on time-averaged axial heat flow. Figure 3 shows the computed time-dependent velocity profiles at different phase angles of the exciting pressure at Womersley numbers equal to 1, 10, and 100. It can be seen that the velocity profile at  $\alpha = 1$  has a quasiparabolic shape at any instant, and is in phase with the stimulating pressure gradient. At high frequency ( $\alpha = 100$ ), the velocity profiles can clearly be divided into two regions: in the vicinity of the wall, the flow shows a typical thin boundary layer of thickness  $\delta = (2\nu/\omega)^{1/2}$ , while in the core region the fluid moves as if it were frictionless slug flow. The phase of the velocity profiles at higher frequencies are shifted about half a period with respect to the stimulating

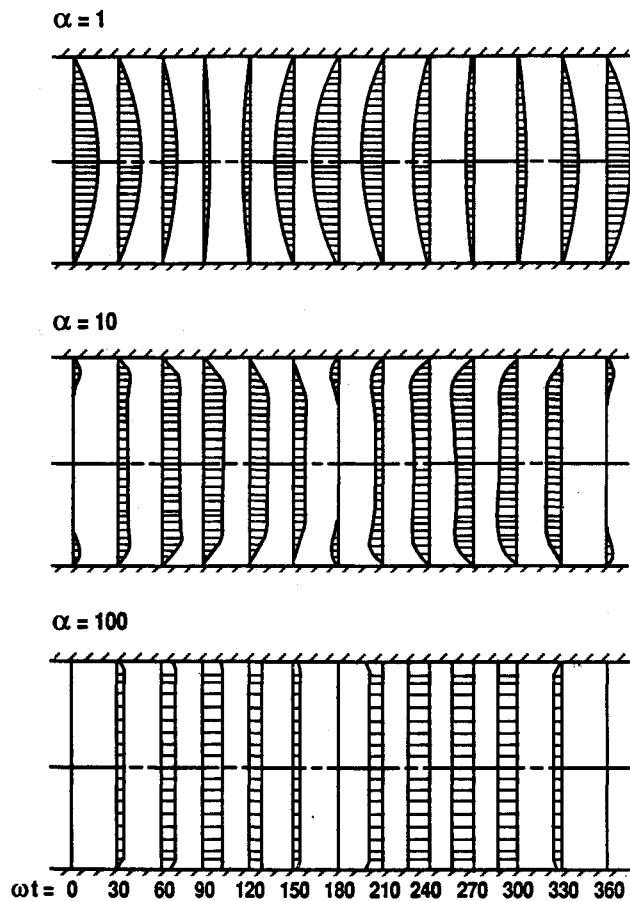


Fig. 3 Computed velocity profiles in oscillating flow for Womersley number  $\alpha = 1, 10$ , and  $100$  at  $\Delta\omega t = 30$ -deg intervals.

pressure gradient. At the intermediate frequency case ( $\alpha = 10$ ), the slug flow boundary is not so evident, but can still be detected.

An alternative representation of the axial velocity profiles are the Lagrangian displacements of the fluid particles at different radial positions within the pipe. Figure 4 shows the trajectories normalized by  $A/\omega^2$  at time intervals of  $\Delta\omega t = 30^\circ$  and at a Womersley number of  $\alpha = 10$ . For this intermediate Womersley number, one can see that the trajectories of the Lagrangian displacement depart considerably from the standard parabolic shape. According to the definition in Eq. (1), the dimensionless tidal displacement  $\Delta x/(A/\omega^2)$  in this case is about 1.8. Note that the dimensionless tidal displacement is a function of Womersley  $\alpha$  only. A comparison of the computed and analytic dimensionless tidal displacement vs Womersley number varying from 0.1 to 100 is shown in Fig. 5. It shows very good agreement with the analytic results given in Ref. 1.

Corresponding to the periodic velocity profiles, the corresponding temperature distribution  $T(x, r, t)$  can be found at any point within the pipe by an evaluation of the energy Equations (4) and (5). Using  $\hat{T} = (T - T_c)/(T_h - T_c)$ , the normalized final periodic temperature distribution shows a nearly linear variation along the pipe with a superimposed time-periodic portion (Fig. 6). This temperature distribution agrees with the assumption made in several analytic studies.<sup>5,8,9</sup> A finite build-up time to this final periodic temperature distribution is required. Figure 7 shows the normalized computed temperature build-up history at  $r = 0$  and  $R_1$  and  $x = L/4$  and  $L/2$  for model 1. For this calculation, the initial temperature in the pipe was assumed to be  $T(r, x, 0) = T_c = 273$  K with  $T(r, 0, t) = T_h = 274$  K. Note that this build-up time can be estimated by  $t_b = \rho c(T_h - T_c)/\phi$ , where  $\phi$  is

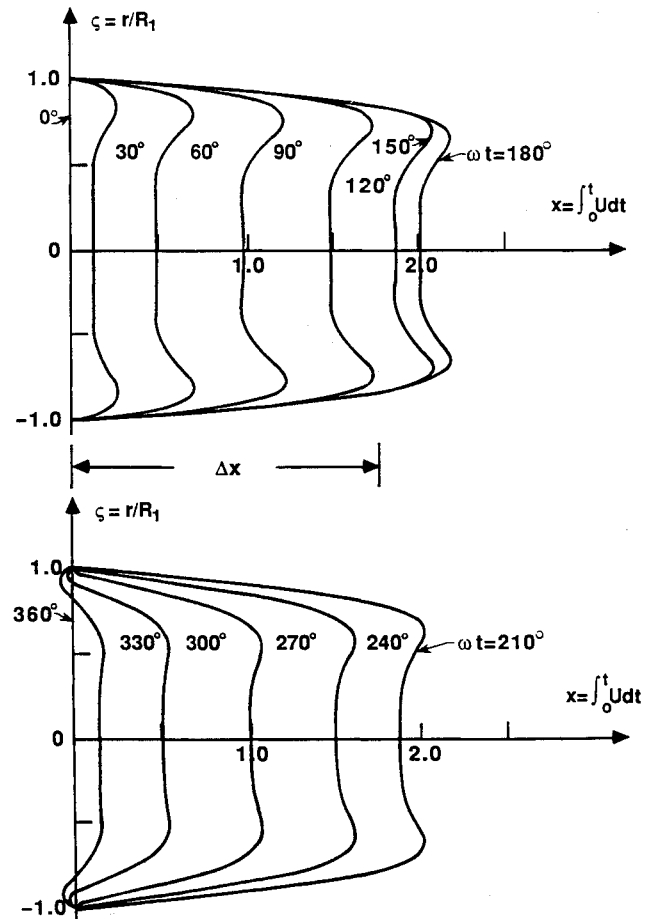


Fig. 4 Normalized Lagrangian displacements at  $\alpha = 10$ .

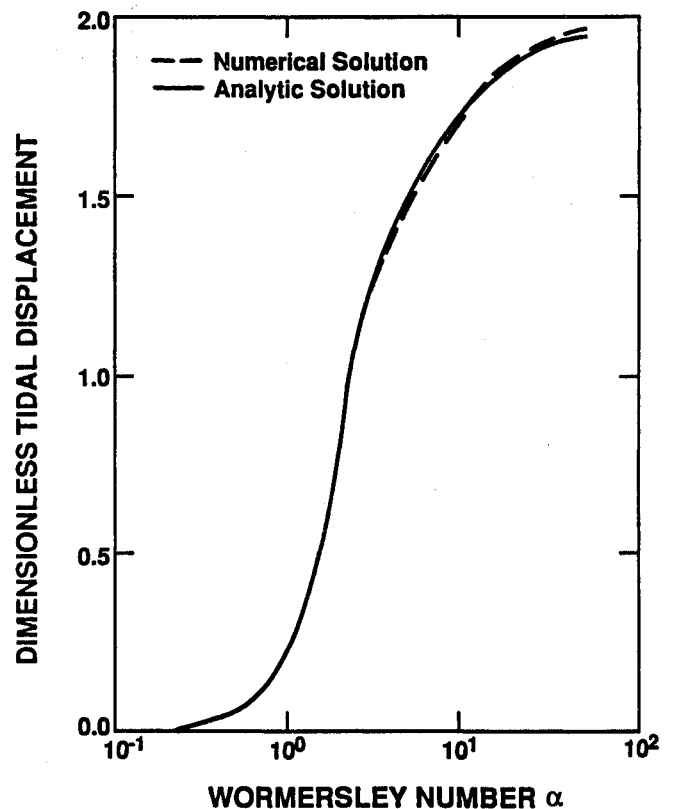


Fig. 5 Dimensionless tidal displacement  $\Delta x$  vs Womersley number  $\alpha$ .

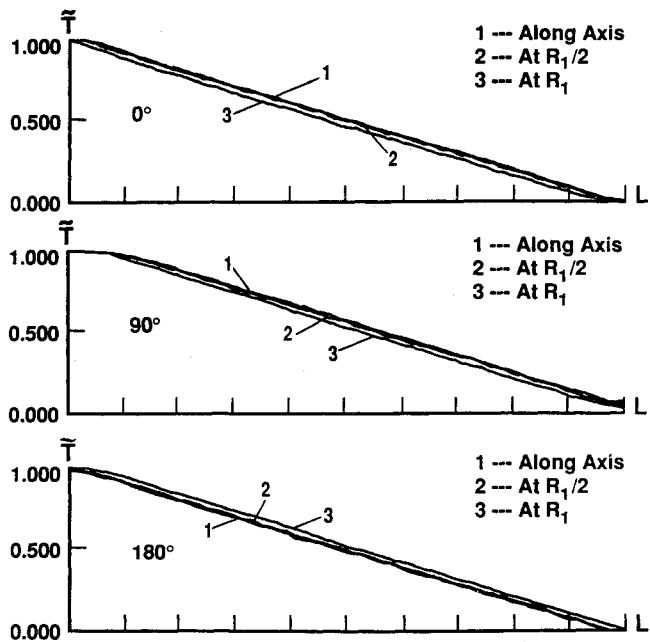


Fig. 6 Normalized temperature distribution in oscillating pipe flow (model 1,  $\alpha = 1$ ,  $R_1 = 0.1$  cm,  $\Delta x = 2$  cm, water-glass).

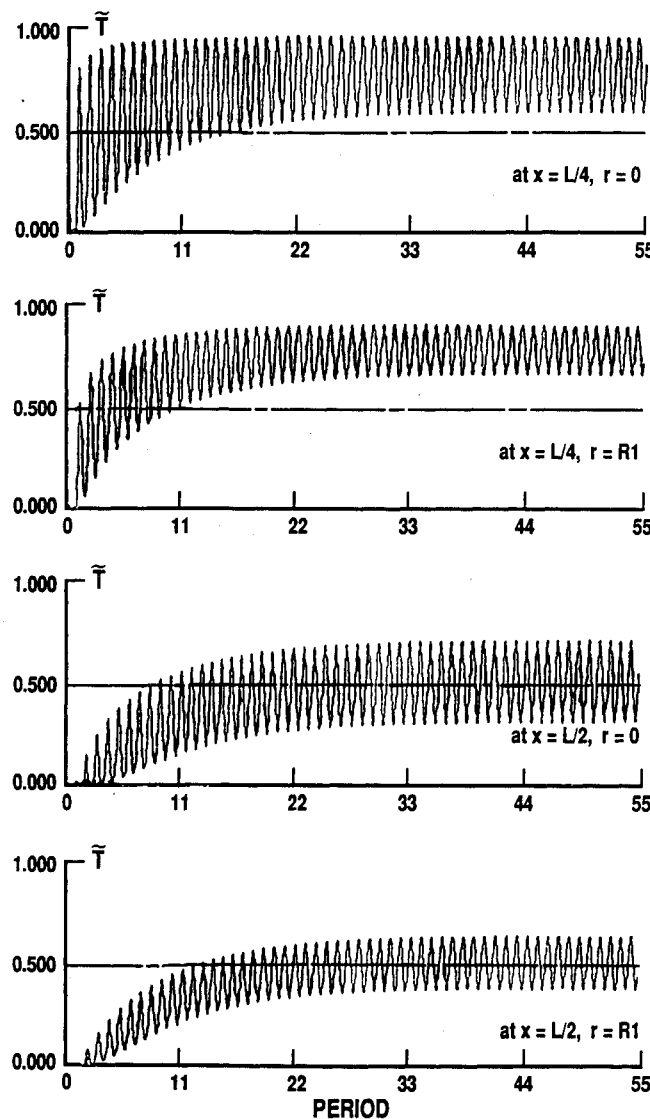


Fig. 7 Normalized temperature build-up process in oscillating pipe flow (model 1,  $\alpha = 1$ ,  $R_1 = 0.1$  cm,  $\Delta x = 5$  cm).

the time-averaged axial heat flux. As already defined in earlier analytical studies,<sup>2,4,5</sup> the time averaged axial heat flux is

$$\phi = \frac{2\rho c}{\tau R_1^2} \int_0^\tau dt \int_0^{R_1} r UT dr \quad (6)$$

where  $\tau$  is the oscillation period. One finds analytically that  $\phi$  is directly proportional to the square of the tidal displacement. Two sets of numerical tests (model 1, at  $x = L/2$ ) were designed to study this “ $\Delta x^{2*}$ ” phenomenon. In the first test, the Wormersley number was set at  $\alpha = 1$ , which is very close to the tuning value for the EAHT process.<sup>2,4</sup> The other case,  $\alpha = 3$ , deviates from this enhanced axial heat tuning point. In both cases, water was the working fluid and glass and steel were chosen as the pipe wall material. The computational results for enhanced axial heat flux  $\phi$  are shown in Fig. 8. One can see that the existence of conducting walls tends to increase heat storage capacity and, hence, enhance the radial and axial heat transfer process. A higher Wormersley number (say,  $\alpha = 3$ ) will generally lead to a larger axial heat flux for fixed tube radius. However, the flux has a maximum near  $\alpha = 1$  when  $\omega$  is fixed but  $R_1$  is allowed to vary. In the present test, for fixed  $R_1$ , the higher Wormersley number simply implies a higher oscillating frequency  $\omega$ . It is pointed out that

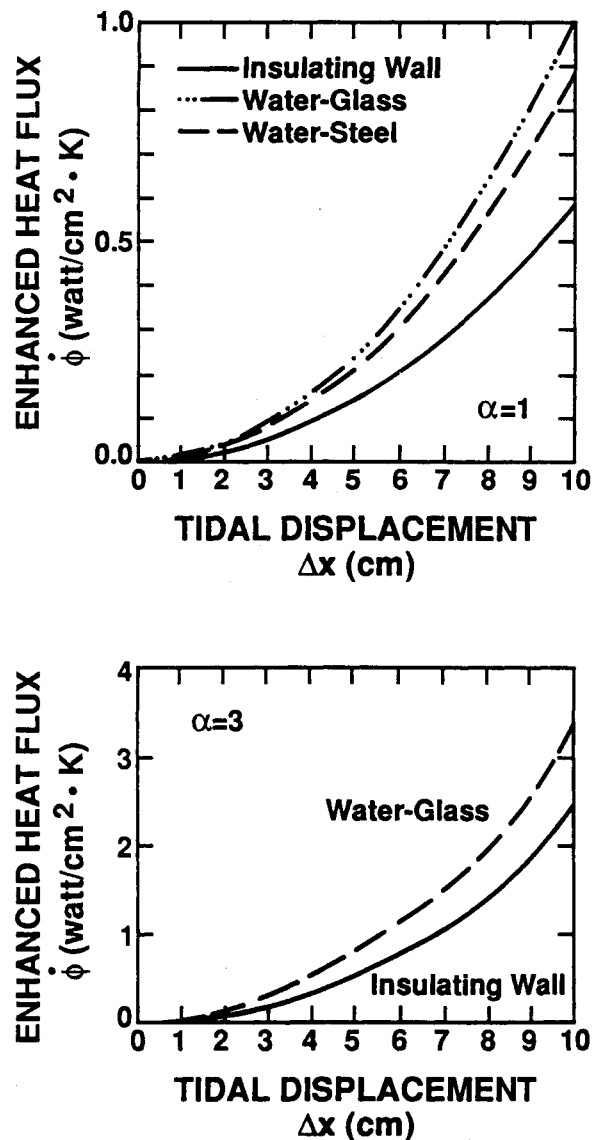


Fig. 8 Heat flux vs tidal displacement.

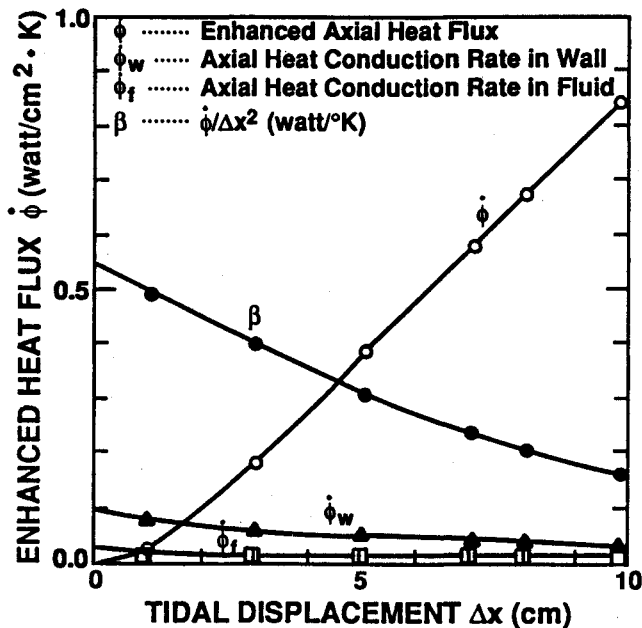


Fig. 9 Comparison of enhanced axial heat flux and axial conductive heat flux at  $\alpha = 3$  for water-glass.

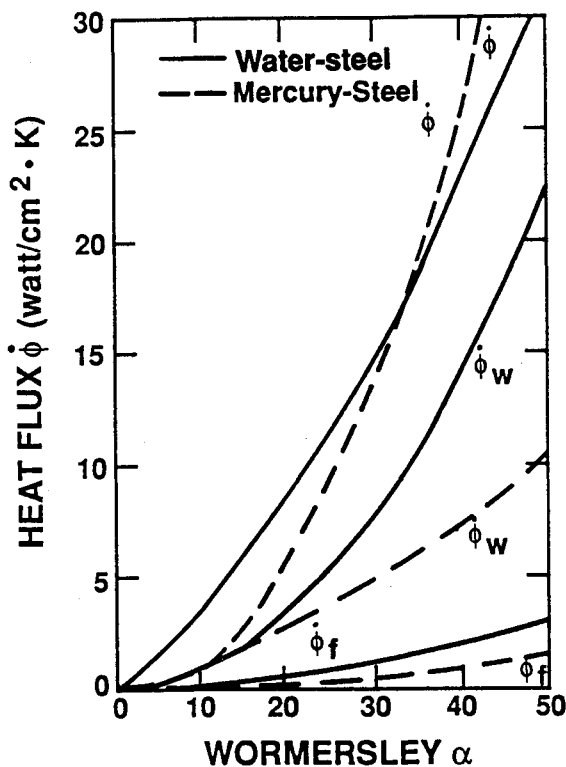


Fig. 10 Variation of heat flux vs Wormersley number ( $\Delta x = 10$  cm).

the enhanced axial heat transfer rate under tuned conditions, according to analytic calculations in tubes of infinite length, increases as the product of  $\omega \Delta x^2$ . This increasing heat transfer rate is accompanied by an increasing input power consumption. For a fixed pipe radius, it is found that the power required to drive the oscillating flow at higher  $\omega$  is proportional to  $\rho \omega^{5/2} \Delta x^2$ , so that the more rapidly increasing power consumption makes the EAHT process inefficient at very high  $\omega$ . However, for cases, such as those shown in Fig. 8, the ratio of power consumed to heat transfer rate is typically less than one percent.

Figure 9 shows the computed enhanced axial heat flux and the axial conductive heat flux in the fluid and wall vs tidal displacement ( $\alpha = 3$ , water-glass) for the end-extended model. Curve  $\phi$  represents the enhanced axial heat flux, and  $\phi_w$  and  $\phi_f$  represent the pure molecular conductive axial heat flux in the wall and in the fluid, respectively. One can clearly see that the  $\phi$  is smaller than  $\phi_w$  or  $\phi_f$ , when the tidal displacement is small; however,  $\phi$  increases very rapidly as the tidal displacement becomes larger. In contrast, the pure axial molecular conductive flux  $\phi_w$  and  $\phi_f$  decline slightly with increasing  $\Delta x$ , due to a weakening of the axial temperature gradient in the central pipe section at large  $\Delta x$ . The ratio of the enhanced heat flux to the square of the tidal displacement is also shown by curve  $\beta$  in Fig. 9. It declines as the tidal displacement increases. This implies that the second power law between the enhanced axial heat flux  $\phi$  and the tidal displacement  $\Delta x$  is weakened if large tidal displacements are used in model 2. This flux reduction is mainly due to the decreased axial temperature gradient in the large displacement case.

The computed enhanced axial heat flux and the pure axial conductive heat flux in the fluid and in the wall vs the Wormersley number, at fixed  $\Delta x = 10$  cm, are shown in Fig. 10. It can be seen that both the enhanced axial heat flux  $\phi$  and pure axial conductive heat flux either in the wall ( $\phi_w$ ) or in the fluid ( $\phi_f$ ) increase as the oscillating frequency gets larger, due to the recovery of the axial temperature gradient. The enhanced axial heat flux is larger than the pure axial conductive heat flux in either case, however, the difference between these two axial heat flows is smaller in the water-steel wall case than in the mercury-steel case. The axial conductive heat flux in the fluid is very much smaller than the enhanced axial heat flux and, hence, is indeed negligible, as is assumed in the theoretical studies of this kind of problem.<sup>1</sup>

It is known that the existence of a conducting wall will, in general, make the EAHT process more efficient, since it creates an additional heat storage capability near the fluid-solid interface.<sup>2</sup> The largest radial distance that the heat can be transported into the wall is defined as wall penetrating thickness  $\delta_w$ , which is a function of the oscillating frequency and the thermal properties of the wall. In view of space limitations and economics, one wants to minimize the capillary wall thickness used in EAHT, yet still be able to make full use of the wall heat storage capacity. If the effective heat flux is defined as the total enhanced axial heat flux over the cross section of the fluid and the solid wall, one can see that the effective heat flux curve first increases with increasing wall thickness  $R_2 - R_1$ , but soon starts to decline as the wall thickness increases further (Fig. 11). For the test case, the optimum wall thickness was found to be about 10% of the pipe diameter.

The variations of the ratio of the enhanced axial heat flux  $\phi$  to the oscillating frequency  $\omega$  in both the water-steel and

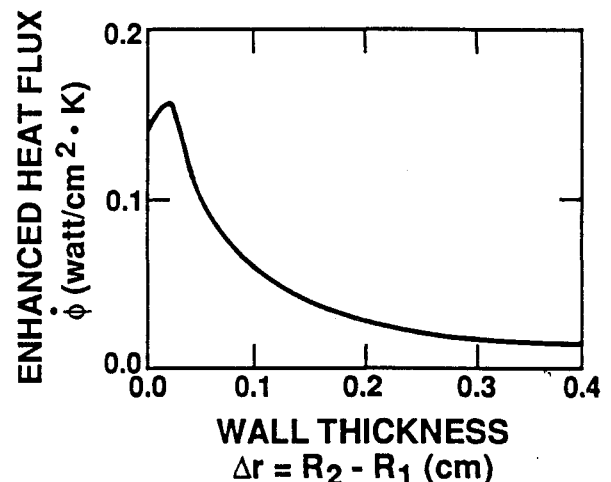


Fig. 11 Influence of wall thickness (model 1, water-glass,  $\alpha = 1$ ,  $\Delta x = 5$  cm).

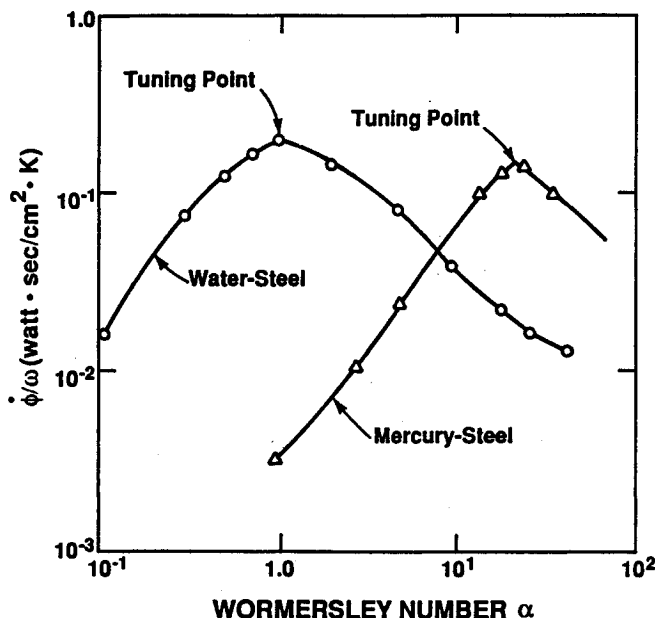


Fig. 12 Tuning curves vs Wormersley number for model 2 at  $\omega = 1$  rad/s and  $\Delta x = 10$  cm.

the mercury-steel wall case for  $\Delta x = 10$  cm are shown in Fig. 12. These curves correspond to axial heat flux at constant frequency, and show the existence of tuning. The optimum Wormersley number is found to equal  $\alpha = 1$  (water-steel,  $Pr = 7.03$ ,  $\omega = 1$  rad/s). This agrees well with the analytical results obtained by Kurzweg.<sup>2</sup> Note that the determination of tuning condition under various combinations of working fluid and wall material is crucial in designing practical EAHT devices, since the optimum enhanced axial heat flux, which is usually orders of magnitude higher than the pure axial conductive heat flux, occurs only near the tuning point for fixed  $\omega$ . For the water-steel case shown in Fig. 12, the optimum pipe radius at  $\omega = 1$  rad/s is  $R_1 = 0.1$  cm. The flux would be  $\phi = 12.8 (T_h - T_c)$  watt/cm<sup>2</sup> under tuned conditions at a frequency of 10 Hz and a tidal displacement of  $\Delta x = 10$  cm for the water-steel combination.

### Concluding Remarks

Enhanced axial heat transfer in oscillating pipe flow for combinations of insulating and conducting walls have been examined numerically. The mechanism of EAHT is that the existing axial temperature gradient is magnified into a very large time-dependent radial temperature gradient by the periodic oscillations. This allows a large amount of heat to be conducted radially and, hence, via axial convection, to be transported between the bounding reservoirs. The effective

axial heat transfer rate can be several orders of magnitude higher than that possible with heat pipes. Unlike existing convective heat transfer methods, this thermal pumping technique involves no net convective mass transfer. This feature of EAHT is especially desirable for those systems in which a large amount of heat must be transferred without an accompanying convective mass exchange, such as, for example, in the cooling system of nuclear reactors.

Extensions of the numerical studies considered here should include: 1) developing a 3D or an axisymmetric 2D model that allows a better approximation of the entire thermal pump system, including reservoirs that also play an important role in this type of heat transfer, and 2) an examination of the role of turbulence at high-frequency  $\omega$  and large tidal displacement  $\Delta x$ , and the associated mass mixing possible for turbulent flow.

### Acknowledgment

Part of the work presented here was funded by a grant from the National Science Foundation under contract number CBT-8611254. This support is gratefully acknowledged.

### References

- <sup>1</sup>Kurzweg, U. H., "Enhanced Heat Conduction in Fluids Subjected to Sinusoidal Oscillations," *Journal of Heat Transfer*, Vol. 107, 1985, pp. 459–462.
- <sup>2</sup>Kurzweg, U. H., "Enhanced Heat Conduction in Oscillating Viscous Flows Within Parallel-Plate Channels," *Journal of Fluid Mechanics*, Vol. 156, 1985, pp. 291–300.
- <sup>3</sup>Kurzweg, U. H., "Temporal and Spatial Distribution of Heat Flux in Oscillating Flow Subjected to an Axial Temperature Gradient," *International Journal of Heat and Mass Transfer*, Vol. 29, No. 12, 1986, pp. 1969–1977.
- <sup>4</sup>Kurzweg, U. H., and Jaeger, M. J., "Tuning Effect in Gas Dispersion under Oscillatory Conditions," *Physics of Fluids*, Vol. 29, 1986, pp. 1324–1326.
- <sup>5</sup>Kurzweg, U. H., and Zhao, L. D., "Heat Transfer by High-Frequency Oscillations: A New Hydrodynamic Technique for Achieving Large Effective Thermal Conductivities," *Physics of Fluids*, Vol. 27, 1984, pp. 2624–2627.
- <sup>6</sup>Taylor, G. I., "Dispersion of Soluble Matter in Solvent Flowing Slowly Through a Tube," *Proceedings of the Royal Society*, London, England, 1953, pp. 186–203.
- <sup>7</sup>Aris, R., "The Dispersion of Solute in Pulsating Flow Through a Tube," *Proceedings of the Royal Society*, A 259, London, England, 1960, pp. 370–376.
- <sup>8</sup>Harris, H. G., and Goren, S. L., "Axial Diffusion in a Cylinder with Pulsed Flow," *Chemical Engineering Science*, No. 22, 1967, pp. 1571–1576.
- <sup>9</sup>Chatwin, P. C., "On the Longitudinal Dispersion of Passive Contaminant in Oscillatory Flow in Tubes," *Journal of Fluid Mechanics*, Vol. 17, Part 3, 1975, pp. 513–527.
- <sup>10</sup>Zhang, J. G., "Time-dependent Enhanced Heat Transfer in Oscillating Pipe Flow," Doctoral Dissertation, Dept. of Aerospace Engineering, Mechanics, and Engineering Science, Univ. of Florida, Gainesville, FL, 1988.